



Antidepressant action of BDNF requires and is mimicked by $G\alpha i1/3$ expression in the hippocampus

John Marshall^{a,1,2}, Xiao-zhong Zhou^{b,c,d,1}, Gang Chen^{e,1}, Su-qing Yang^{b,c}, Ya Li^{b,c}, Yin Wang^{b,c}, Zhi-qing Zhang^{b,c}, Qin Jiang^f, Lutz Birnbaumer^{g,h,2}, and Cong Cao^{b,c,f,i,2}

^aDepartment of Molecular Pharmacology, Physiology, and Biotechnology, Brown University, Providence, RI 02912; ^bJiangsu Key Laboratory of Neuropsychiatric Diseases Research, Soochow University, Suzhou 215000, China; ^cInstitute of Neuroscience, Soochow University, Suzhou 215000, China; ^dDepartment of Orthopedics, The Second Affiliated Hospital of Soochow University, Suzhou, 215004 Jiangsu, China; ^eDepartment of Neurosurgery, The First Affiliated Hospital of Soochow University, Suzhou, 215006 Jiangsu, China; ^fThe Fourth School of Clinical Medicine, The Affiliated Eye Hospital, Nanjing Medical University, 210029 Nanjing, China; ^gNeurobiology Laboratory, National Institute of Environmental Health Sciences, Research Triangle Park, NC 27709; ^hSchool of Medical Sciences, Institute of Biomedical Research, Catholic University of Argentina, C1107AAZ Buenos Aires, Argentina; and ⁱNorth District, The Municipal Hospital of Suzhou, Suzhou 215001, China

Contributed by Lutz Birnbaumer, February 14, 2018 (sent for review December 26, 2017; reviewed by William N. Green and Elizabeth A. Jonas)

Stress-related alterations in brain-derived neurotrophic factor (BDNF) expression, a neurotrophin that plays a key role in synaptic plasticity, are believed to contribute to the pathophysiology of depression. Here, we show that in a chronic mild stress (CMS) model of depression the $G\alpha i1$ and $G\alpha i3$ subunits of heterotrimeric G proteins are downregulated in the hippocampus, a key limbic structure associated with major depressive disorder. We provide evidence that $G\alpha i1$ and $G\alpha i3$ ($G\alpha i1/3$) are required for the activation of TrkB downstream signaling pathways. In mouse embryonic fibroblasts (MEFs) and CNS neurons, $G\alpha i1/3$ knockdown inhibited BDNF-induced tropomyosin-related kinase B (TrkB) endocytosis, adaptor protein activation, and Akt–mTORC1 and Erk–MAPK signaling. Functional studies show that $G\alpha i1$ and $G\alpha i3$ knockdown decreases the number of dendrites and dendritic spines in hippocampal neurons. In vivo, hippocampal $G\alpha i1/3$ knockdown after bilateral microinjection of lentiviral constructs containing $G\alpha i1$ and $G\alpha i3$ shRNA elicited depressive behaviors. Critically, exogenous expression of $G\alpha i3$ in the hippocampus reversed depressive behaviors in CMS mice. Similar results were observed in $G\alpha i1/G\alpha i3$ double-knockout mice, which exhibited severe depressive behaviors. These results demonstrate that heterotrimeric $G\alpha i1$ and $G\alpha i3$ proteins are essential for TrkB signaling and that disruption of $G\alpha i1$ or $G\alpha i3$ function could contribute to depressive behaviors.

depression | BDNF | $G\alpha i1$ | $G\alpha i3$ | hippocampus

The neurotrophin BDNF (brain-derived neurotrophic factor) and its high-affinity tropomyosin-related kinase B (TrkB) receptor play a critical role in synaptic plasticity and memory (1). Alterations in BDNF levels have been reported to result in major depressive disorder (2). The hippocampus is one of several limbic brain structures implicated in the pathophysiology and treatment of depression (3–5). Stress, a risk factor for depression, can result in neuronal atrophy (6) characterized by reduced synaptic connections (7). Human studies and animal models support a “neurotrophin hypothesis” of depression proposing that depression is associated with reduced expression and/or function of BDNF in depressive states (8), which can be alleviated with antidepressant therapy (3–5).

Depression has also been reported to disrupt TrkB receptor downstream signaling (9). Binding of BDNF to TrkB results in its dimerization and tyrosine autophosphorylation and subsequent recruitment of adaptor proteins (10–14) that link TrkB to the activation of MAPK (11, 13, 15) and the PI3K–Akt–mammalian target of rapamycin (mTOR) pathways (10, 14, 15). Increasing evidence shows that the inhibitory alpha subunits of heterotrimeric guanine nucleotide-binding proteins ($G\alpha i$ proteins) play a key role in growth factor signaling (16, 17). $G\alpha i$ proteins were originally identified by their ability to inhibit adenylyl cyclase and are members of four subclasses, Gs, Gi/o, Gq, and G12/13; the Gi/o includes $G\alpha i$ (3), Go (2), and transducins (18). The $G\alpha i$ subclass of heterotrimeric G proteins includes the highly similar $G\alpha i1$, $G\alpha i2$, and $G\alpha i3$

proteins encoded by the genes *GNAI1*, *GNAI2*, and *GNAI3*, respectively, with more than 94% sequence identity between $G\alpha i1$ and $G\alpha i3$ (19). Our studies have demonstrated that $G\alpha i1$ and $G\alpha i3$ (but not $G\alpha i2$) are required for EGF- and keratinocyte growth factor (KGF)-induced Akt–mTOR complex 1 (mTORC1) activation (16, 20). In the current study, we show that $G\alpha i1$ and $G\alpha i3$ ($G\alpha i1/3$) are required for BDNF-induced TrkB receptor signaling and the regulation of depressive behaviors.

Results

Double Knockout of $G\alpha i1$ and $G\alpha i3$ Inhibits BDNF-Induced Akt–mTORC1 and Erk Activation in Mouse Embryonic Fibroblasts. Mouse embryonic fibroblasts (MEFs) have been reported to express TrkB receptors and provide a valuable cell system to examine the underlying mechanisms of BDNF signaling (21). To begin to address the role of $G\alpha i$ proteins in TrkB signaling, we utilized a $G\alpha i1$ and $G\alpha i3$ double-knockout (DKO) MEF cell line (16, 20). Depletion of $G\alpha i1$ and $G\alpha i3$ in the DKO MEFs was confirmed by Western blot analysis (Fig. 1A), whereas $G\alpha i2$ expression was intact. TrkB

Significance

Heterotrimeric $G\alpha i$ proteins are known to transduce G protein-coupled receptor signals. We have identified a role for $G\alpha i$ proteins in mediating brain-derived neurotrophic factor (BDNF)–tropomyosin-related kinase B (TrkB) signaling. BDNF dysfunction contributes to the pathophysiology of depression. In a stress model of depression $G\alpha i1$ and $G\alpha i3$ proteins are downregulated in the hippocampus, a limbic structure associated with major depressive disorder. We show that $G\alpha i1/G\alpha i3$ proteins are required for TrkB downstream signaling, and knockout mice exhibited severe depressive behaviors with decreased dendritic morphology. Established stress-induced depressive behavior is corrected by intrahippocampal expression of $G\alpha i3$. These results demonstrate that heterotrimeric $G\alpha i1$ and $G\alpha i3$ proteins are essential for TrkB signaling and that disruption of $G\alpha i1$ or $G\alpha i3$ function could contribute to depressive behaviors.

Author contributions: J.M., Q.J., L.B., and C.C. designed research; X.-z.Z., G.C., S.-q.Y., Y.L., Y.W., Z.-q.Z., and C.C. performed research; L.B. contributed new reagents/analytic tools; J.M., X.-z.Z., G.C., S.-q.Y., Y.L., Y.W., Z.-q.Z., Q.J., L.B., and C.C. analyzed data; and J.M., Q.J., L.B., and C.C. wrote the paper.

Reviewers: W.N.G., University of Chicago; and E.A.J., Yale University School of Medicine.

The authors declare no conflict of interest.

Published under the [PNAS license](#).

See Commentary on page 3742.

¹J.M., X.-z.Z., and G.C. contributed equally to this work.

²To whom correspondence may be addressed. Email: John_Marshall@Brown.edu, birnbau1@gmail.com, or caocong@suda.edu.cn.

This article contains supporting information online at www.pnas.org/lookup/suppl/doi:10.1073/pnas.1722493115/-DCSupplemental.

Published online March 5, 2018.

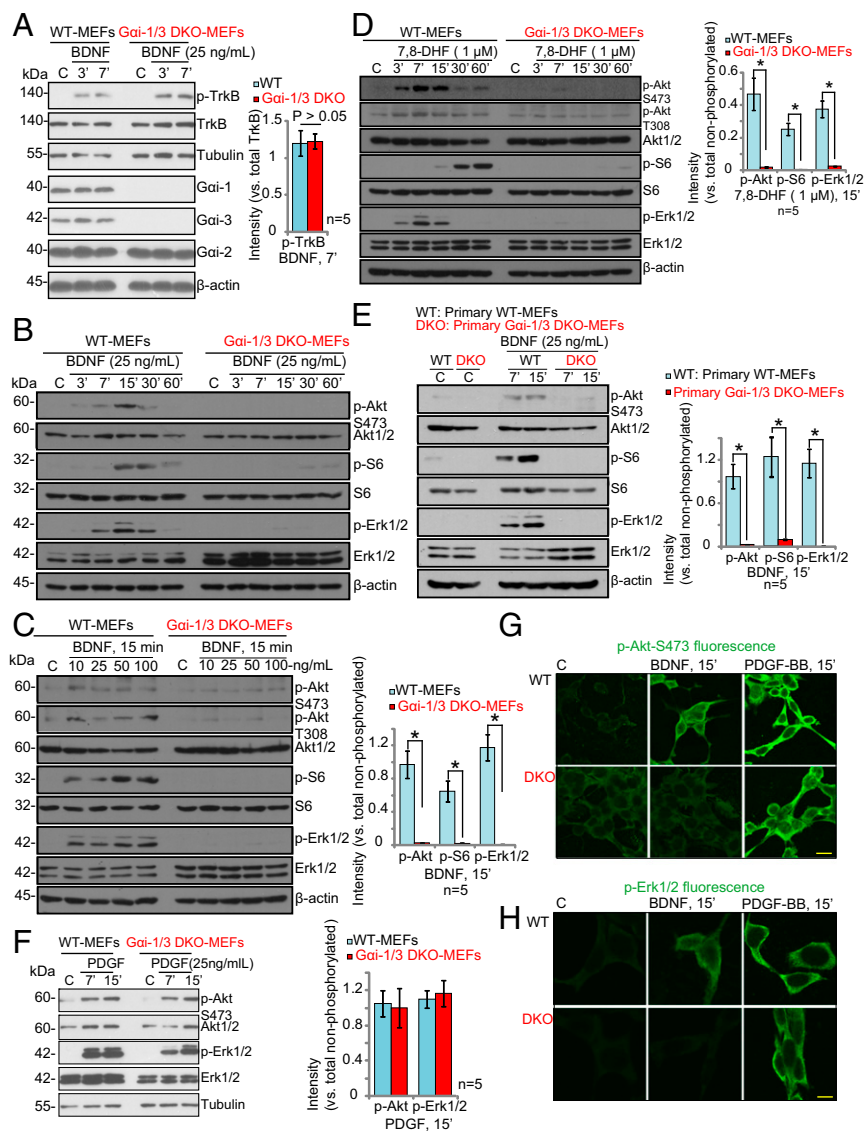


Fig. 1. *Gai1* and *Gai3* DKO blocks BDNF-induced Akt-mTORC1 and Erk activation in MEFs. (A–F) WT or *Gai1/3*-DKO MEFs were treated with BDNF (applied at the indicated concentrations for the indicated times) or with PDGF-BB (25 ng/mL) and were analyzed by Western blotting for the listed proteins. For Western blot assays, equal amounts of quantified protein lysates were loaded (30 μ g per treatment) or the same set of lysate samples was run on identical gels. The indicated proteins were quantified using ImageJ software (A, C–E, and F; $n = 5$). * $P < 0.001$ by Student's t test. Data are reported as mean \pm SD. (G and H) Immunofluorescence analysis was performed to test p-Akt (G) and p-Erk1/2 (H). (Scale bars: 10 μ m.)

expression and BDNF-induced TrkB phosphorylation were comparable in WT and DKO MEFs. Significantly, BDNF-induced phosphorylation of Akt (at Ser-473 and Thr-308), S6 (Ser-235/236), and Erk1/2 (Tyr202/Thr-204) was significantly reduced in *Gai1/3*-DKO MEFs ($P < 0.001$ vs. WT MEFs) (Fig. 1B and C), suggesting that *Gai1* and *Gai3* are required for Akt-mTORC1 and Erk-MAPK activation. In agreement with previous studies (16, 20), the expression of total Akt, S6, and Erk1/2 was equal in WT and DKO MEFs (Fig. 1B and C). Furthermore, 7,8-Dihydroxyflavone (7,8-DHF), a selective TrkB agonist (22, 23), induced phosphorylation of Akt, S6, and Erk1/2 in WT MEFs but not in the DKO MEFs (Fig. 1D). In confirmation of the results in the MEF cell line, we tested isolated primary cultures of *Gai1/3*-DKO MEFs (16) and found that BDNF-induced Akt-mTORC1 and Erk-MAPK activation was similarly abolished (Fig. 1E), whereas PDGF-BB (25 ng/mL)-induced phosphorylation of Akt and Erk1/2 was unaffected (Fig. 1F). Immunofluorescence imaging further confirmed that BDNF-induced but not PDGF-BB-induced phosphorylation of Akt and Erk1/2 was blocked in *Gai1/3*-DKO MEFs (Fig. 1G and H).

***Gai1* and *Gai3* Have Redundant Roles in BDNF-Induced Akt-mTORC1 and Erk Activation in MEFs.** To investigate whether depleting *Gai1* or *Gai3* individually would disrupt BDNF signaling, *Gai* single-

knockout (SKO) MEFs were utilized (16, 20). BDNF-induced phosphorylation of Akt (Ser-473 and Thr-308), S6 (Ser-235/236), and Erk1/2 (Tyr202/Thr-204) was only partially decreased in *Gai1*- or *Gai3*-SKO MEFs ($P < 0.01$, vs. WT MEFs) (Fig. 2A) and was intact in *Gai2*-SKO MEFs ($P > 0.05$, vs. WT MEFs) (Fig. 2B), whereas *Gai1* and *Gai3* DKO resulted in complete inhibition of BDNF signaling (Fig. 2A). These results suggest that expression of either *Gai1* or *Gai3* can take part in TrkB signaling. To demonstrate that expression of either *Gai1* or *Gai3* is sufficient for BDNF signaling, we tested whether exogenous expression of *Gai1* or *Gai3* would rescue signaling in DKO MEFs (16, 20). As shown in Fig. 2C, the exogenous expression of *Gai1* or *Gai3* in DKO MEFs was sufficient to restore BDNF-induced Akt and Erk activation. To exclude possible off-target effects from the genetically modified MEFs, we employed a siRNA strategy to knock down the *Gai* protein in WT MEFs. As shown in Fig. 2D, single knockdown of *Gai1* or *Gai3* by targeted siRNA in the WT MEFs resulted in a weak but significant inhibition of BDNF-induced phosphorylation of Akt, S6, and Erk1/2. In contrast, BDNF stimulation of WT MEFs depleted of both *Gai1* and *Gai3* using the CRISPR/Cas9 system showed complete inhibition of Akt, S6, and Erk1/2 phosphorylation ($P < 0.001$ vs. control cells) (Fig. 2D).

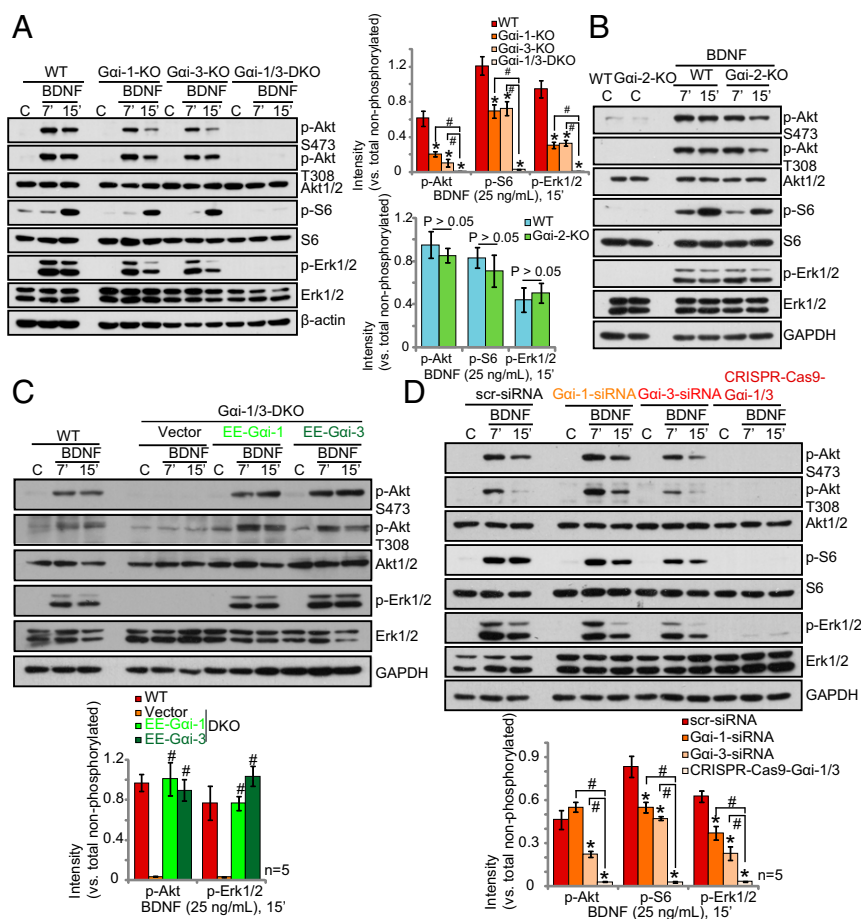


Fig. 2. *Gai1* and *Gai3* are required for BDNF-induced Akt-mTORC1 and Erk activation in MEFs. (A and B) WT MEFs, *Gai1*- or *Gai3*-SKO MEFs, *Gai2*-SKO MEFs, and *Gai1/3*-DKO MEFs were treated with BDNF (25 ng/mL) for the indicated time and were analyzed by Western blot for the listed proteins. (C) DKO MEFs were transiently transfected with plasmids encoding EE-*Gai1*-cDNA, EE-*Gai3*-cDNA, or empty vector. MEFs were treated with BDNF (25 ng/mL) for the indicated time and were tested by Western blot for the listed proteins. (D) WT MEFs were transfected with 100 nM of scr-siRNA, *Gai1*, or *Gai3* siRNA, and MEFs stably expressing CRISPR/Cas9-*Gai1* and CRISPR/Cas9-*Gai3* were treated with BDNF (25 ng/mL) and were tested by Western blot for the listed proteins. * $P < 0.01$ vs. WT MEFs (A) and vs. scr-siRNA (D). # $P < 0.001$ (A and D). # $P < 0.001$ vs. vector (C).

***Gai1/3* Are Required for TrkB Adaptor Complex Formation.** TrkB autophosphorylation provides docking sites for adaptor proteins and the recruitment of downstream signaling molecules (24). We next examined whether depletion of *Gai1/3* would interfere with adaptor protein complex formation. BDNF-activated TrkB recruits the adaptor protein Shc, which in turn recruits Grb2. Grb2 then associates with Grb2-associated binder 1 (*Gab1*) to activate PI3K and downstream Akt-mTORC1 signaling (15). SHP2 recruitment is required for downstream MEK-Erk activation and is essential for neurite outgrowth and branching (25). We found that loss of *Gai1/3* in DKO MEFs abolished BDNF-induced TrkB recruitment and phosphorylation of adaptor proteins, including Shc and SHP2 (Fig. 3A) and *Gab1* (Fig. 3B). Significantly, *Gai3* was also part of the complex with Grb2, *Gab1*, and SHP2 (Fig. 3B). In agreement with the reduced recruitment of *Gab1*, BDNF-induced phosphorylation of *Gab1*, whose activation is required for downstream PI3K-Akt and Erk-MAPK activation, was inhibited in *Gai1/3*-DKO MEFs (Fig. 3C) and in WT MEFs transfected with shRNA (Fig. 3D). *Gai1* or *Gai3* SKO inhibited *Gab1* phosphorylation by BDNF, whereas *Gai2* KO failed to affect *Gab1* activation (Fig. 3C and E). Reexpression of *Gai1* or *Gai3* in the DKO MEFs restored *Gab1* phosphorylation (Fig. 3F). In agreement with previous studies (25, 26), BDNF-induced phosphorylation of Akt, S6, and Erk1/2 was severely inhibited in *Gab1*-KO MEFs (Fig. 3G), in confirmation of the important role played by *Gab1* in TrkB signaling.

***Gai1/3* Are Required for BDNF-Induced TrkB Signaling in Cerebellar Granule Neurons.** In primary cerebellar granule neurons, BDNF signaling is required for migration (27) and survival (28). To examine the effect of neuronal knockdown of *Gai1/3* expression on BDNF signaling, primary murine cerebellar granule neurons were infected with lentiviral constructs expressing shRNA for

Gai1 and *Gai3* or a scrambled shRNA. Infection of neurons with lentiviral shRNA resulted in a 95% reduction of *Gai3* expression and an 80% reduction of *Gai1* expression (Fig. 4A). BDNF-induced phosphorylation of Akt, S6, and MEK1/2-Erk1/2 was greatly diminished in cerebellar granule neurons with *Gai1/3* shRNA ($P < 0.001$ vs. neurons with scrambled control shRNA) (Fig. 4A, Right).

To determine if *Gai1/3* proteins can be recruited to TrkB, we performed a coimmunoprecipitation assay. Results demonstrate that *Gai3* (Fig. 4B) and *Gai1* (Fig. 4D) coimmunoprecipitate with TrkB in response to BDNF in cerebellar granule neurons. BDNF-induced TrkB immunoprecipitation with SHP2 and *Gab1* was blocked by *Gai1/3* shRNA (Fig. 4B). Consequently, phosphorylation of SHP2 and *Gab1* in response to BDNF was largely inhibited (Fig. 4C). We also found that TrkB coimmunoprecipitated with APPL1 (a pleckstrin homology domain, phosphotyrosine-binding domain, and leucine zipper motif 1) (Fig. 4D), which is known to associate with TrkB and is required for signal transduction (29). These results in primary neurons, together with the MEF data, support a role for *Gai* proteins in BDNF-induced TrkB adaptor complex formation and downstream signal transduction.

***Gai1/3* Are Required for BDNF Signaling and for Dendrite and Spine Formation in Hippocampal Neurons.** To investigate the potential function of *Gai1/3* in primary hippocampal neurons, we knocked down *Gai1/3* expression using lentiviral shRNA. After coinfection of hippocampal neurons with *Gai1* shRNA lentivirus plus the *Gai3* shRNA lentivirus, we observed a significant reduction in the protein levels of *Gai1* (over 95%) and *Gai3* (over 80%), as evaluated by immunoblotting (Fig. 5A, Left). Consequently, BDNF-induced phosphorylation of *Gab1*, Akt, S6, and Erk1/2 was inhibited by *Gai1/3* shRNA (Fig. 5A). TrkB expression and

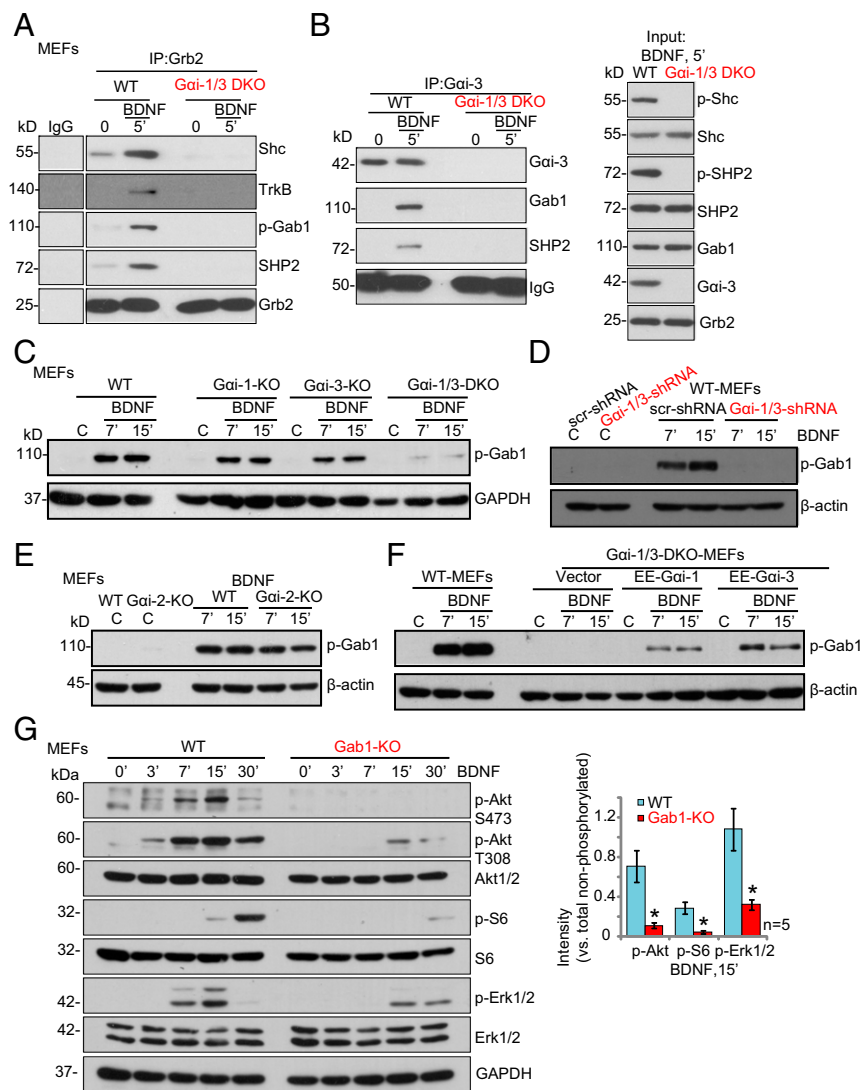


Fig. 3. *Gai1/3* are required for the TrkB adaptor complex formation. (A and B) WT and *Gai1/3*-DKO MEFs were treated with BDNF (25 ng/mL) for 5 min, and the association among TrkB, *Gai3*, and adaptor proteins was tested by the immunoprecipitation assay. Input control shows the expression of listed proteins in the total cell lysates. (C–E) WT MEFs, *Gai1*- or *Gai3*-SKO MEFs, and *Gai1/3*-DKO MEFs (C), WT MEFs or *Gai1/3* MEFs transfected with shRNA or scr-shRNA (D), and WT and *Gai2*-KO MEFs were treated with BDNF and p-Gab1 and were tested by Western blot analysis. β -Actin served as the loading control. (F) DKO MEFs were transiently transfected with vector encoding EE-*Gai1*-cDNA, EE-*Gai3*-cDNA, or empty vector, and BDNF (25 ng/mL)-induced Gab1 phosphorylation was analyzed by Western blot. (G) WT or *Gab1*-KO MEFs were treated with BDNF (25 ng/mL) for the indicated time and were analyzed by Western blotting for the listed proteins. * $P < 0.001$ vs. WT MEFs.

BDNF-induced TrkB phosphorylation were equivalent in control GFP neurons and *Gai1/3* shRNA neurons (Fig. 5A, Right). Significantly, TrkB endocytosis by BDNF was blocked by *Gai1/3* shRNA (Fig. 5A, Right), whereas EGF receptor (EGFR) surface levels were unaffected.

BDNF-TrkB activation is critical for hippocampal neuron development (30, 31), including dendritic outgrowth and spine formation (32). To examine whether knockdown of *Gai1/3* expression alters the morphology of hippocampal neurons, we infected hippocampal neurons at day 5 in vitro (DIV 5) with lentiviral *Gai1* and *Gai3* shRNA. The lentiviral vector coexpresses GFP under the control of a CMV promoter, allowing detection of transduced cells. For spine density and morphology analyses, neurons were fixed after 5 d, and anti-GFP immunocytochemistry was performed. As shown in Fig. 5B, the number of secondary dendrites extending from the pyramidal primary dendrite, the number of dendritic spines in each hippocampal neuron, and the length of each dendrite were significantly decreased by *Gai1/3* shRNA (Fig. 5B and C). However, the soma area was unaffected (Fig. 5C).

To confirm these results in vivo, lentiviral *Gai1* and *Gai3* shRNA (sh*Gai1/3*) were microinjected into the hippocampus of mice. Microinjection of lentivirus effectively infected hippocampal neurons, as shown by GFP immunostaining 7 d post-injection (Fig. 5D), and substantially decreased expression levels of *Gai1* and *Gai3* (Fig. 5E). Significantly, infection with either sh*Gai1* or sh*Gai3* decreased p-Akt and p-Erk1/2 signaling (Fig.

5E), while coinfection with sh*Gai1* and sh*Gai3* further inhibited p-Akt and p-Erk1/2 levels (Fig. 5E). TrkB expression and phosphorylation were unaffected by lentiviral sh*Gai* infection (Fig. 5E). Using immunostaining for GFP to reveal neuronal morphology, we examined the effects of *Gai1/3* knockdown on dendrite number and spine density in hippocampal sections. Single infection with either sh*Gai1* or sh*Gai3* decreased the number of secondary dendrites (Fig. 5F and G) and dendritic spines (Fig. 5H and I), while coinfection with sh*Gai1* and sh*Gai3* had the greatest detrimental effect (Fig. 5G and I). The number of hippocampal pyramidal neurons was unaffected by lentivirally mediated shRNA *Gai1/3* knockdown (Fig. 5G).

***Gai1/3* Knockdown in the Hippocampus Produces Depressive Behavior.**

Chronic mild stress (CMS), a model of depression (33–35), decreases the expression of BDNF in the hippocampus, and this decreased expression is believed to contribute to dendrite and spine deficits in depression (36). We investigated whether CMS exposure could affect *Gai1/3* expression in the brain. CMS exposure for 14–56 d led to a significant decrease of *Gai1* and *Gai3* expression in the hippocampus (Fig. 6A) but not in the cortex (Fig. 6B), suggesting that *Gai1* and *Gai3* down-regulation could be associated with depressive behaviors. To test this hypothesis, we examined the consequences of bilateral hippocampal injection of lentiviral *Gai1* and *Gai3* shRNA on depression- and anxiety-like behaviors. Results show that *Gai1* shRNA or *Gai3* shRNA injection into the

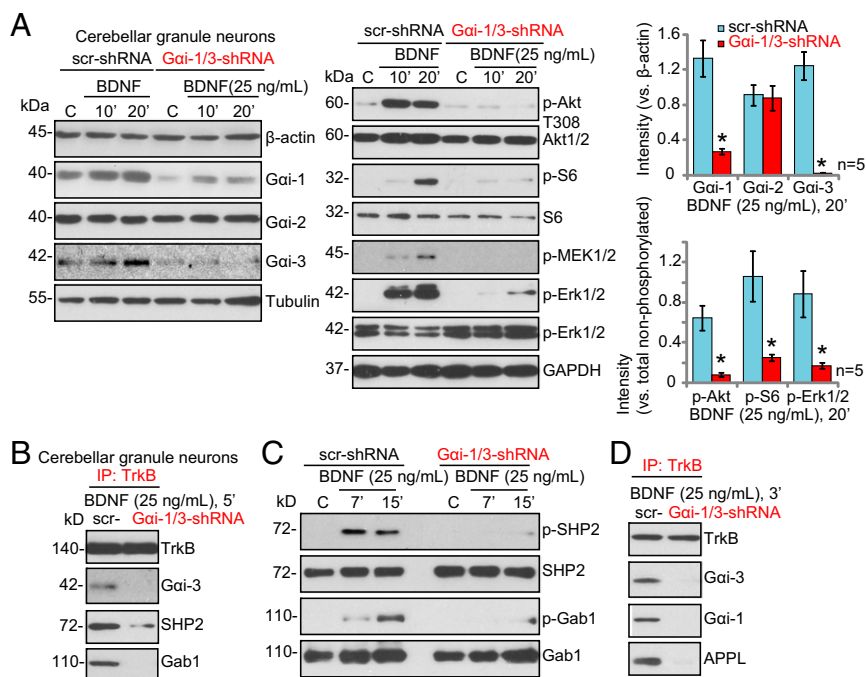


Fig. 4. Gai1/3 are required for BDNF-induced signaling and TrkB adaptor complex formation in cerebellar granule neurons. (A and C) Lentiviral-mediated shRNA knockdown of Gai1/3 disrupts downstream signaling. Primary cultured cerebellar granule neurons transduced with lentiviral Gai1 shRNA plus Gai3 shRNA or scr-shRNA for 24 h were treated with BDNF (25 ng/mL), and Akt, S6, MEK1/2–Erk1/2, SHP2, and Gab1 phosphorylation was analyzed by Western blotting. (B and D) Lentiviral-mediated shRNA knockdown of Gai1/3 decreases the association between TrkB and Gai1/3, SHP2, APPL1, and Gab1. Primary cerebellar granule neurons transduced with Gai1 shRNA plus Gai3 shRNA or scr-shRNA were stimulated with BDNF (25 ng/mL), and the association was tested by immunoprecipitation. * $P < 0.001$ vs. scr-shRNA.

hippocampus elicited depressive behaviors in which mice exhibited significantly longer immobility times in both a forced swim test (FST) ($P < 0.001$ vs. GFP control) (Fig. 6D) and a tail-suspension test (TST) ($P < 0.001$ vs. GFP control) (Fig. 6E). In a sugar-preference test, in which anhedonic behavior is inferred by a reduced preference for sugar water, mice showed decreased preference after hippocampal injection of Gai1 or Gai3 shRNA ($P < 0.001$ vs. GFP control) (Fig. 6F). Furthermore, coinjection of Gai1 shRNA and Gai3 shRNA lentivirus into the hippocampus intensified depressive behaviors (Fig. 6D–F) compared with the injection of Gai1 shRNA or Gai3 shRNA alone (Fig. 6D–F).

Based on the above results, we hypothesized that exogenous Gai overexpression in the hippocampus would induce anti-depressive behavior. To test this, we performed bilateral stereotaxic delivery of an adenovirus–Gai3 construct (Ad-Gai3) into the hippocampi of treatment-naïve adult animals and assessed FST and TST behaviors. Immunoblotting of hippocampal tissue confirmed exogenous Gai3 expression in the hippocampus (Fig. 6G), and p-Akt and p-Erk1/2 levels were increased in the Ad-Gai3-infected hippocampus (Fig. 6H), while TrkB and p-TrkB levels were unchanged (Fig. 6G). Behavioral testing at 7 d postinjection showed that mice receiving the Ad-Gai3 injection exhibited a significantly reduced duration of immobility in both the FST ($P < 0.001$ vs. Ad-GFP control) (Fig. 6I) and the TST ($P < 0.001$ vs. Ad-GFP control) (Fig. 6J).

If hippocampal Gai down-regulation is the cause of CMS-induced depression in mice, rather than a secondary effect, then restoring Gai expression should prevent depressive behavior. To test this hypothesis, we exogenously expressed Gai3 by bilateral Ad-Gai3 delivery into the hippocampus. Exogenous expression Gai3 reversed CMS-induced depressive behavior (Fig. 6K–M). These results support the hypothesis that the level of Gai1/3 expression in the hippocampus regulates TrkB signaling to influence depressive behavior.

Severe Depressive-Like Behaviors in Gai1/3-DKO Mice. To confirm the role of Gai1/3 in depression, we generated Gai1/3-DKO mice. Western blotting of hippocampal lysates confirmed that Gai1 and Gai3 were depleted in the DKO mice, whereas Gai2 was unaffected (Fig. 7A). TrkB expression and phosphorylation were equivalent in WT and DKO mice (Fig. 7A). However, p-Akt and p-Erk1/2 were decreased in the DKO mice (Fig.

7A). In behavioral testing, the DKO mice displayed depressive behaviors, with significantly increased immobility times in both the FST (Fig. 7B) and the TST (Fig. 7C) ($P < 0.001$ vs. WT mice). The DKO mice also exhibited a reduction in their preference for sugar ($P < 0.001$ vs. WT mice).

To examine the morphology of hippocampal CA1 neurons, GFP-expressing control lentivirus was microinjected into the hippocampus of DKO mice, and anti-GFP immunostaining was performed on sections 7 d postinjection. Analysis of confocal images of GFP antibody-stained neurons revealed that DKO mice displayed a reduced number of hippocampal pyramidal neurons ($P < 0.001$ vs. WT mice) (Fig. 7E and F). We also observed a severe reduction in dendrite complexity, as indicated by a reduction in the number of secondary dendrites extending from the pyramidal primary dendrite ($P < 0.001$ vs. WT mice, 40 neurons per group) (Fig. 7G). Furthermore, the number of dendritic spines was significantly reduced in the DKO mice ($P < 0.001$ vs. WT mice, 40 neurons per group) (Fig. 7H and I), whereas mean spine width was not significantly different between WT and DKO mice ($P > 0.05$ vs. WT mice) (Fig. 7J). These results show that knockout of Gai1/Gai3 disrupts BDNF signaling, hypothesized to be required for the maintenance of pyramidal neuron morphology and the prevention of depressive behaviors.

Discussion

Gai proteins are well known to transduce signals between G protein-coupled receptors and their effectors (18). The major finding of this study is the unconventional role of Gai1 and Gai3 proteins in mediating downstream BDNF–TrkB signal transduction. The results suggest that Gai1 and Gai3 have redundant roles in TrkB signaling, as depletion of both Gai1 and Gai3 was required to completely block BDNF signaling (Figs. 2A and 5E), although disruption of Gai3 had a greater impact. In hippocampal neurons, Gai3 knockdown more significantly reduced BDNF signaling (Fig. 5E) and dendrite morphology (Fig. 5G and I). Furthermore, CMS decreased Gai3 expression more than Gai1 expression (Fig. 6A), and Gai3 knockdown produced larger depressive effects (Fig. 6D–F).

In cerebellar and hippocampal neurons, in response to BDNF, Gai1 or Gai3 are recruited to TrkB (Fig. 4D) and are required for TrkB adaptor protein association (Fig. 4B) and downstream signaling (Figs. 4A and 5A). Gai1 or Gai3 proteins do not appear

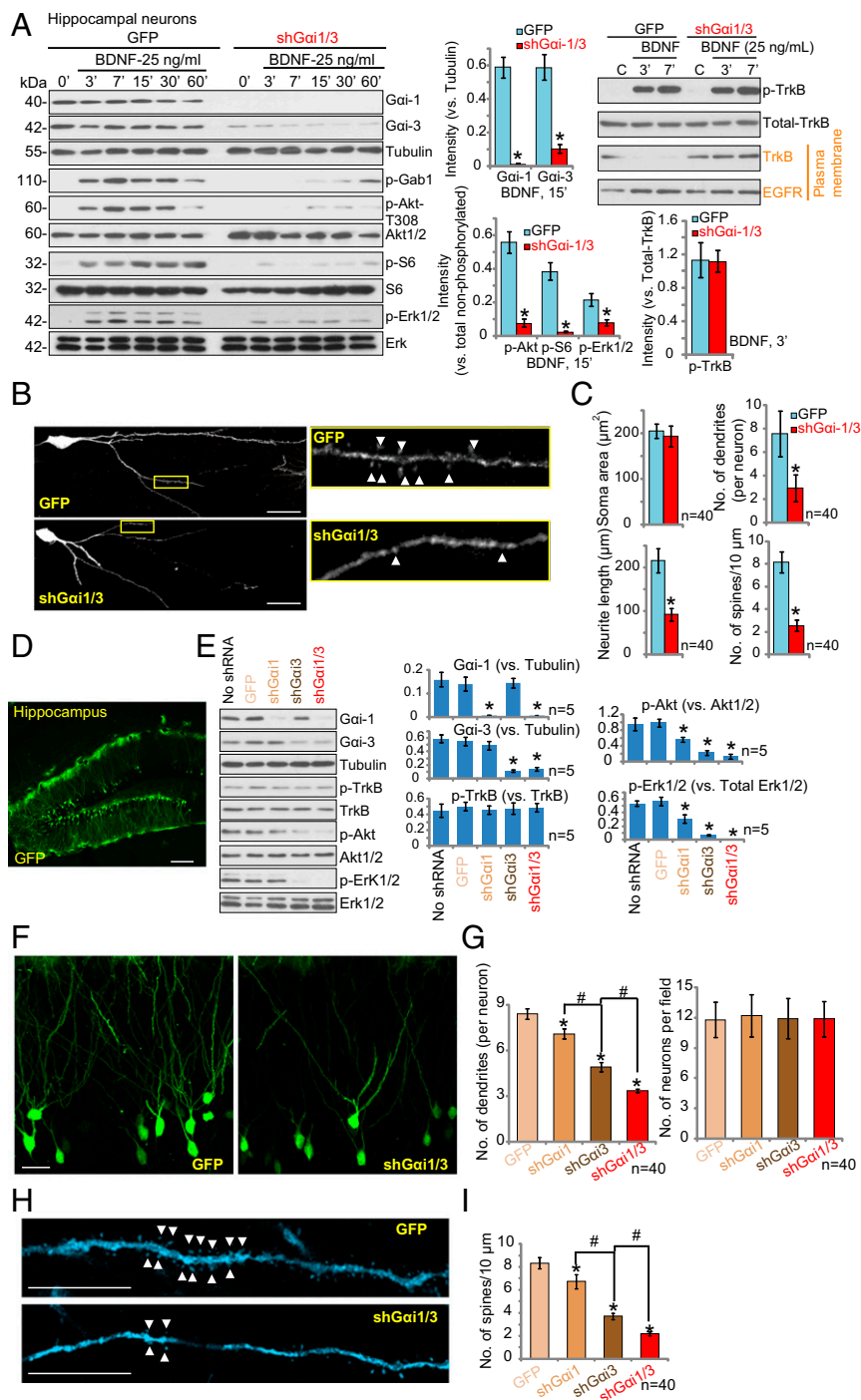


Fig. 5. Gai1/3 are required for BDNF signaling, endocytosis, and dendrite outgrowth in the hippocampal neurons. (A) Lentiviral-mediated shRNA knockdown of Gai1/3 disrupts downstream TrkB signaling and TrkB endocytosis in primary hippocampal neurons. Hippocampal neurons were infected with lentiviral Gai1 shRNA plus lentiviral Gai3 shRNA (shGai1/3) or a lentiviral scr-shRNA for 24 h. Neurons were stimulated with BDNF (25 ng/mL) and analyzed for the listed proteins in total and cell-surface lysates. (B and C) Lentiviral-mediated shRNA Gai1/3 knockdown decreases dendrite morphology in primary hippocampal neurons. On day 5 after infection, neurons were stained for GFP expression (encoded by the lentiviral shRNA vectors), and the morphology of hippocampal neurons was quantified. (B) Representative images of anti-GFP staining are presented. Arrowheads indicate spines. (Scale bars: 25 μm ; magnification: *Inset*, 6.8 \times .) (C) Dendrite length, branching, soma area, and the number of dendritic spines were quantified. For spine analysis, 30- μm -long dendritic segments (50–80 μm from soma) were selected, and spines from 40 neurons were counted. (D) A representative image of GFP expression 7 d after hippocampal injection of a lentiviral GFP control virus shows a high efficiency of infection. (E) Intrahippocampal lentiviral shRNA-mediated knockdown of Gai1/3 decreases Akt and Erk1/2 activity, as analyzed by Western blotting with phospho-specific antibodies. Hippocampi were isolated and tested by Western blotting of listed proteins ($n = 5$). (F–I) Intrahippocampal lentiviral shRNA-mediated knockdown of Gai1/3 decreases the formation of secondary dendrites and spines. (F and H) Representative images showing hippocampal neuron morphology are presented for control and shRNA Gai1/3-infected neurons stained for GFP. Arrowheads in H indicate spines. (Scale bars: 25 μm in F and 5 μm in H.) (G) The number of neurons and dendrites per neuron were counted. (I) Spines were counted from 30- μm -long dendritic segments (50–80 μm from soma) of 40 randomly selected neurons. * $P < 0.001$ vs. GFP. # $P < 0.001$.

to influence TrkB autophosphorylation but act downstream of TrkB and upstream of Gab1, resulting in phosphorylation of Gab1, SHP2, and Shc. Knockdown of Gai1/Gai3 inhibits BDNF-induced Gab1 activation and downstream PI3K–Akt–mTOR and Erk–MAPK activation. Our group reported a similar function for Gai1 and Gai3 in mediating EGFR signal transduction (16). Importantly, knockdown of Gai1/3 blocks TrkB endocytosis in response to BDNF (Fig. 5A), providing insight into the mechanism by which Gai1/3 exhibits such a dominant effect on TrkB signaling. TrkB retrograde signaling is critical in the regulation of BDNF-induced survival and differentiation of neurons in the CNS (37–40). Significantly, we found that knockdown of Gai1/3 disrupts the association of TrkB with the membrane adaptor

protein APPL1 (Fig. 4D). Previous studies have reported that APPL1 binds to membrane receptors, including TrkA and TrkB, in endosomal fractions (41). APPL1 endosomes may serve as platforms for the assembly of TrkB adaptor signaling complexes regulating the Akt–mTORC1 and Erk–MAPK pathways (29, 41, 42). It is possible Gai1/3 proteins play a role in TrkB sorting into distinct endosomal compartments essential for the activation of specific signaling cascades that modulate synapse formation and survival and the differentiation of neurons in the CNS.

BDNF is a key mediator of activity-dependent dendrite formation (43, 44) via PI3K and MAPK signaling (45). In support of the role for Gai1/3 in BDNF signaling, Gai1/3 knockdown in hippocampal neurons in vitro (Fig. 5C) and in vivo (Fig. 5F and

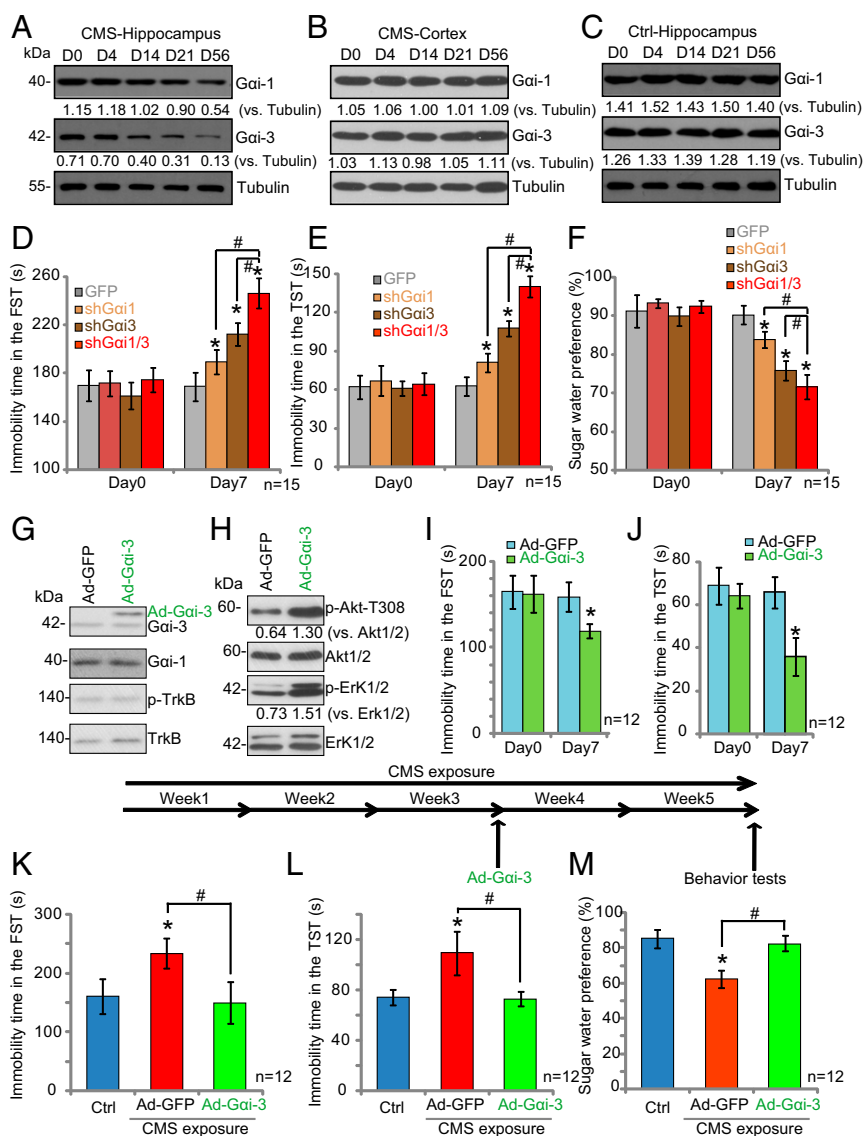


Fig. 6. Gai1/3 knockdown in the hippocampus produces depressive behaviors. (A–C) CMS exposure decreases Gai1 and Gai3 expression in the hippocampus. Western blot analysis of Gai1 and Gai3 expression in the hippocampus (A) and cortex (B) of mice exposed to the CMS model for 14–56 d compared with control hippocampus (C). (D–F) Gai1 shRNA or Gai3 shRNA injection into the hippocampus elicited depressive behaviors. Immobility times in the FST (D) and TST (E) and sucrose water preference (F) were examined on day 7 after intrahippocampal injection of GFP or lentiviral Gai1 shRNA and/or Gai3 shRNA. (G–J) Exogenous Gai3 expression in the hippocampus induces antidepressive behavior. On day 7 after intrahippocampal injection of Ad-GFP or Ad-Gai3, immobility times in the FST (I) and TST (J) were tested, and then hippocampi were isolated and analyzed by Western blotting of the listed proteins (G and H). (K–M) Exogenous expression of Gai3 reversed CMS-induced depressive behavior. The immobility times in the FST (K) and TST (L) and sucrose water preference (M) were tested in control and CMS mice with or without intrahippocampal injection of Ad-GFP or Ad-Gai3. * $P < 0.001$ vs. GFP (D–F, I, and J). * $P < 0.001$ vs. control mice (K–M). # $P < 0.001$ (D–F and K–M).

G) disrupted dendritic branching. BDNF is also required for the maintenance of mature synaptic spines, and blocking BDNF reduces spine density (46). In accordance, Gai1/3 knockdown decreased the number of hippocampal dendritic spines in vitro (Fig. 5C) and in vivo (Fig. 5H and I). Significantly, in vivo knockdown of Gai1/3 resulted in fairly rapid (within 7 d) morphological changes. Consistent with this observation, BDNF treatment has been shown to rapidly (within 24 h) regulate dendrite morphology (45) and spine density in hippocampal neurons (47–49). Depression is associated with a decrease in hippocampal spine density (50), and rapid BDNF-induced changes in dendrite complexity and spine density have been linked to the mechanism of fast-acting antidepressants (51, 52).

Given the role of BDNF signaling in the neuropathology of anxiety and depression, we examined if Gai expression was associated with depression. Using the CMS model, we found a significant down-regulation of Gai1 and Gai3 expression in the hippocampus (Fig. 6A). Furthermore, mice subjected to lentiviral shRNA Gai1/3 knockdown in the hippocampus and Gai1/3-DKO mice presented with severe depressive-like behaviors, as indicated by prolonged immobility times in the FST and TST and decreased sugar preference (Fig. 6D–F). Conversely, virally mediated expression of exogenous Gai3 in the hippocampus prevented the antidepressive-like behaviors

induced by CMS (Fig. 6K–M). Last, using the CRISPR-Cas9 method, we generated Gai1/3-DKO mice, which exhibited depressive-like behavior identical to that demonstrated by mice with virally mediated hippocampal Gai1/3 knockdown (Fig. 7).

BDNF deficiency is implicated in depression, and antidepressant drugs act to restore BDNF levels (53). The administration of the selective serotonin-reuptake inhibitor fluoxetine prevents stress-induced atrophy of dendrites and spines (54), and reduction of TrkB receptor signaling attenuates the antidepressant structural and behavioral actions of fluoxetine (55). Interestingly, in a postnatal mouse model, fluoxetine induced depression-like behaviors (56) that were associated with a decline in hippocampal Gai1 (Gnai1) gene expression, as well as mTOR, protein kinase C gamma, and hyperpolarization-activated cyclic nucleotide-gated channel 1, via HDAC4-mediated transcriptional repression (56). Fluoxetine rescue of behavior was accompanied by normalization of Gai1, Hdac4, and mTOR expression (56).

In summary, our results suggest a model in which Gai1/3 proteins are required for BDNF-induced TrkB signaling. In response to BDNF, Gai1 or Gai3 associates with TrkB, resulting in TrkB internalization and endosomal trafficking, which is required for adaptor protein association and downstream signaling. In behavioral models of depression, the levels of Gai1 and

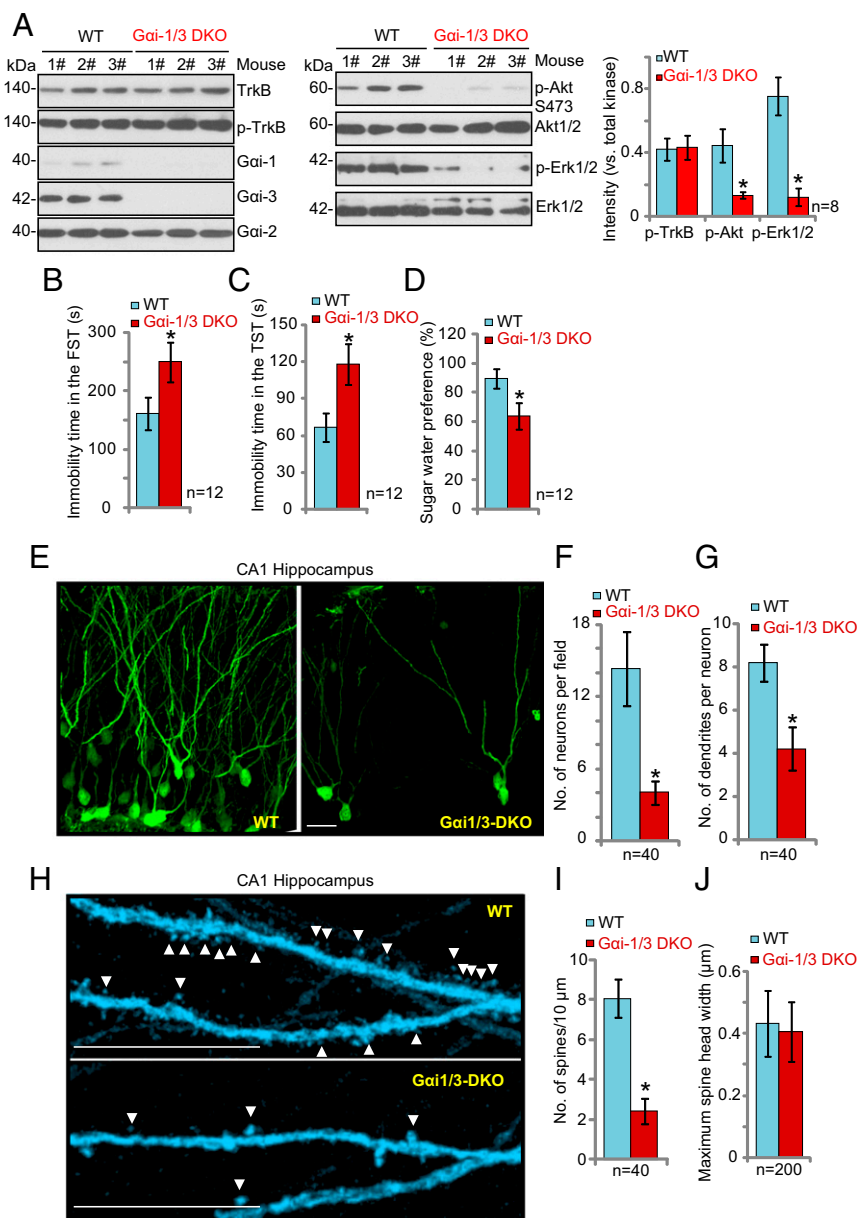


Fig. 7. Severe depressive-like behaviors in *Gai1/3*-DKO mice. (A) Depletion of *Gai1* and *Gai3* in the DKO mice disrupts signaling. The expression of the listed proteins in the CA1 hippocampus of WT and *Gai1/3*-DKO mice was examined by Western blot analysis. (B–D) DKO mice display depressive behaviors. For both WT and *Gai1/3*-DKO mice, the FST (B), TST (C), and sucrose water preference test (D) were performed. (E–J) Analysis of DKO hippocampal CA1 neuronal morphology. (E and H) Representative images of CA1 pyramidal hippocampal neuronal morphology. Arrowheads indicate spines. (Scale bars: 25 μm in E and 5 μm in H.) (F) The number of neurons in randomly selected 200 × 200 μm fields was counted. (G and I) The number of secondary dendrites (G) and spines (I) in 40 random neurons were counted. Spines were analyzed from 30-μm-long apical dendritic segments (50–80 μm from soma). (J) The maximum spine width of 200 spines from 10 randomly selected neurons was measured by Image J software. **P* < 0.001 vs. WT mice.

Gai3 are down-regulated, resulting in reduced BDNF signaling, atrophy of dendrites, and loss of dendritic spines in hippocampal neurons. The results support the hypothesis that a reduction of *Gai1* or *Gai3* contribute to depression and suggest that antidepressants mediate their therapeutic benefit, in part, by increasing levels of *Gai1* or *Gai3* in the hippocampus. Finally, other neurotrophic/growth factors, including VEGF, have been implicated in the pathophysiology of depression (57), and *Gai1/Gai3* could also play a role in their signal transduction.

Materials and Methods

Reagents and Antibodies. BDNF and PDGF-BB were provided by Calbiochem. Puromycin was purchased from Sigma-Aldrich. The cell-culture reagents were provided by Gibco BRL. Tubulin, Erk1/2, Akt1/2, GSK3β, Shp2, Shc, Gab1, Grb2, *Gai1*, *Gai2*, *Gai3*, goat anti-rabbit IgG-HRP, and goat anti-mouse IgG-HRP antibodies were obtained from Santa Cruz Biotechnology, and the mouse β-actin monoclonal antibody was from Sigma. p-Akt (Ser-473), p-Akt (Thr-308), p-Gab1 (Tyr-627), p-S6K (Thr-389), p-S6 (Ser-235/236), p-GSK3α/β (Ser21/9), p-Erk1/2 (Thr-202/Tyr-204), and p-MEK1/2 antibodies were purchased from Cell Signaling Technology. TrkB and p-TrkB antibodies were purchased from Abcam.

MEFs. WT, *Gai1/3*-DKO, and *Gai1*-, *Gai2*-, and *Gai3*-SKO MEFs and WT and *Gab1*-KO MEFs were described previously (16, 20, 58).

Cerebellar Granule Neuron Culture. As described (59), cerebella were removed from 5-d-old mouse pups and placed in ice-cold HBSS, pH 7.4, with penicillin/streptomycin. Cerebella were diced into small chunks before incubation in 10 mL of trypsin (0.5 mg/mL) in HBSS at 37 °C for 10 min (with agitation every 2–3 min), followed by the addition of serum to stop protease digestion. Any chunks were pelleted and resuspended three times in growth medium [DMEM, 10% horse serum, 25 mM KCl, glucose (6 g/L), 2 mM glutamine plus 10 U penicillin and streptomycin]. The supernatant containing the dissociated cells was plated (2 million cells per well in six-well plates) into growth medium on laminin (Invitrogen)-coated plates.

***Gai1* and *Gai3* shRNA/siRNA of MEFs in Vitro.** Lentivirus with shRNA targeting murine *Gai1* (sc-41751-V; Santa Cruz Biotechnology) or murine *Gai3* (sc-37255-V; Santa Cruz Biotechnology) were added for 18 h. For stable cell lines, MEFs infected with the lentiviral *Gai1/3* shRNA were selected with puromycin (1.0 μg/mL). The culture medium was replaced with fresh puromycin-containing culture medium every 2 d until resistant colonies were formed (7–8 d). Control MEFs or neurons were infected with scramble nonsense shRNA lentiviral particles or lentiviral GFP (Santa Cruz).

Primary Murine Hippocampal Neuron Culture and shRNA. Hippocampal cultures were prepared using a modified Banker culture protocol (60). Briefly, hippocampi from mice at postnatal d 4 (P4) were dissected, dissociated in a papain-enzyme solution (30 min at 37 °C), and plated into six-well plates at a density of 165 cells/mm² on poly-L-lysine-coated coverslips and were grown in Neurobasal plating medium containing B27 purchased from Invitrogen, penicillin/streptomycin, and 10% FBS. The lentiviral shRNA vectors PGLV3/U6/GFP/Puro (encoding a GFP marker under the control of a CMV promoter) expressing *Gai3* shRNA (5'-AGATGATGCCCGACAGTGA-3') or the murine *Gai1* shRNA (5'-GAGGAGTGAAGCAGTACAAG-3') were generated by GenePharma. For in vitro studies, hippocampal neurons at DIV 5 were infected with lentiviral *Gai1* shRNA plus lentiviral *Gai3* shRNA (sh*Gai1/3*) or the lentiviral scrambled control shRNA (scr-shRNA, with GFP) (multiplicity of infection: 8). Five days after transfection (at DIV10), neurons were fixed, permeabilized, and labeled with a rabbit polyclonal anti-GFP (1:1,000; ab290; Abcam). The secondary antibody was goat anti-rabbit Dylight 488 (1:1,000). A confocal laser-scanning microscope (LSM700, Zeiss) was utilized to analyze the GFP staining. Forty randomly selected neurons per condition were analyzed for soma area and for dendrite number and length with ImageJ software (NIH). For each measurement, at least 40 neurons from randomly selected 200 × 200 μm fields were counted. Spines were counted from 30-μm-long dendritic segments 50–80 μm from soma.

Transient Expression of *Gai* Proteins. The constructs with EE-tagged *Gai1* and EE-tagged *Gai3* have been described previously (16, 20). Plasmids were transfected using Lipofectamine 2000 (Invitrogen).

CRISPR/Cas9 Knockout of *Gai1* and *Gai3* in Vitro. The CRISPR/Cas-9 plasmids with single-guide RNAs (sgRNAs) targeting murine *Gai1* and *Gai3* were purchased from Santa Cruz Biotechnology (*Gai1*: sc-420596-ACT; *Gai3*: sc-420598-ACT). Both *Gai1* and *Gai3* CRISPR plasmids and the homology-directed repair plasmid (Santa Cruz) were transfected into MEF cells using Lipofectamine 2000 (Invitrogen) and were selected with puromycin. Control cells were treated with the empty vector with control sgRNA (Santa Cruz Biotechnology).

Confocal Immunofluorescence Microscopy of MEFs. MEFs and neuronal cultures were fixed and stained for confocal immunofluorescence microscopy as described (61).

Generation of *Gai1/3*-DKO Mice. All animal procedures were approved by the Institutional Review Board (IRB) of Soochow University (Suzhou, China). The generation of *Gai*-KO mice by the CRISPR-Cas9 method was performed by GenePharma. The superovulation of the C57/B6 donor female mice was performed by the administration of pregnant mare chorionic gonadotrophin (CG) followed by the injection of 5 IU of human CG after 48 h. Female mice were mated with male mice, and fertilized eggs were subjected to microinjection the following day. Microinjection of sgRNA (targeting mouse *Gnai1* or *Gnai3*) and Cas9 mRNA was performed as described (62). The embryonic-modified mice were born 19–20 d after the microinjection. At P7 the newborn mice (F0) were genotyped, and *Gnai1* or *Gnai3* SKO was further characterized. The female chimeric *Gnai*^{+/−}-SKO mice at week 4–5 were again mated with WT male mice, and newborn (P7) mice (G1) were genotyped. We identified several positive *Gnai*-KO mice, indicating that the CRISPR-Cas9 genome modification had been integrated into the germ cells and that the *Gnai*-SKO mouse line had been established. *Gnai1*-SKO and *Gnai3*-SKO mice were crossed to achieve *Gnai1/Gnai3*-DKO mice. Two murine *Gnai1* sgRNA sequences were tested: TCGACTTCGGAGACTCTGCT (target 1) and CCATCATTAGAGCCATGGGG (target 2); two murine *Gnai3* sgRNA sequences were tested: TTTTATAGCGCTGGAGAACTCTGG (target 1) and CATTGCAATCATACGAGCCATGG (target 2). In both cases, target 1 successfully induced *Gnai* SKO. Primers for genotyping are *Gnai1*: sense, GGTGAGTGAAGAGCCTACGG/antisense, CACAGCGACTGGACCTCAA and *Gnai3*: sense, GGAGGGTTGCTTATGGAAT/anti-sense, ACCTAACACTTCAAAAACAGA.

Intrahippocampal Lentivirus Administration. Lentivirus was purchased from GenePharma. Adult male C57/B6 mice (6–7 wk old) were anesthetized using a mixture of ketamine and xylazine, and the lentiviral *Gai1* shRNA and/or *Gai3* shRNA was bilaterally microinjected into the CA1 region (1 μL per side with an infusion rate of 0.25 μL/min) with a viral titer of 3 × 10⁸ transduction units/mL. The coordinates targeting dorsal mouse hippocampal CA1 were as follows: anteroposterior, −1.94 mm; lateromedial, −1.40 mm; and dorsoventral, −1.35 mm, relative to the bregma. Seven days after the hippocampal injection of lentivirus, hippocampi were sectioned coronally (30-μm thickness) on a freezing microtome. Sections were heated at 85 °C for 5 min in an antigen-unmasking solution (Biyuntian) and were blocked with 3% normal goat serum, 0.3% (wt/vol) Triton X-100, and 0.1% BSA at 22–25 °C for 1 h. The sections were incubated with a rabbit polyclonal anti-GFP

(1:1,000; ab290; Abcam). The secondary antibody was goat anti-rabbit Dylight 488 (1:400; Jackson ImmunoResearch). A confocal laser-scanning microscope (LSM700, pinhole 0.5; Zeiss) was utilized to analyze the GFP staining with Imaris 7.3.0 software (Bitplane). Hippocampal neurons were analyzed for soma number and dendrite branching. For each measurement, at least 40 neurons were counted from randomly selected 200 × 200 μm fields. Spine numbers were counted manually from a 30-μm-long segment of a dendrite that was 50–80 μm away from soma. Spine head width, defined as the maximum width of the spine head, was measured using ImageJ software. At least 10 neurons and 20 spines per neuron were analyzed.

For adenovirus production *Gai3* was amplified by RT-PCR. The primer sequences were as follows: P1, 5'-AGGTCGACTCTAGAGGATCCCGCCACCACGGCTGCACGTTGAGCGCCG-3'; P2, 5'-CAACTTAAAGGAATGTGGCTTTATGTATGGACTACAAGGA-3'. The PCR fragment was subcloned into the BamHI/Agel site of the pDC315-Flag plasmid to produce pDC315-*Gai3* with Flag fused to the C terminus of *Gai3*. HEK293 cells were transfected with the pDC315-*Gai3*-Flag using Lipofectamine 2000 and the pBHGloxΔE1,3 Cre plasmid (GenePharma) as the helper plasmid to generate the recombinant adenovirus Ad-*Gai3*-Flag, and the supernatant was harvested after 1 wk. After viral amplification (3×), the supernatant was purified using an Adeno-X Virus Purification kit (Clontech). To titer the virus, serially diluted adenovirus was used to transduce HEK293 cells. After 1 wk, the labeled HEK293 cells were counted to calculate the viral titer (2.5 × 10¹⁰ pfu/mL).

CMS Depression Model. As described (63), the CMS procedure involves the sequential application of a variety of mild stressors, including forced-swim, restraint, water and food deprivation, housing in wet sawdust, light/dark cycle reversal, and housing in constant illumination or darkness (33, 34). The CMS lasted for a total of 3 wk; a detailed protocol is provided in Table S1.

TST. Mice were suspended by the tail, using adhesive scotch tape, to a hook in a soundproof box. The test session was videotaped and observed by two individual observers (35, 63). The total duration of immobility during a 6-min test was calculated in seconds. Data collected were expressed as mean immobility time in seconds ± the SD.

FST. Each experimental mouse was forced to swim in an open cylindrical container (diameter, 16 cm; height, 25 cm) with a 20-cm depth of water at 23–24 °C; the total duration of immobility (35, 63) during a 5-min FST was scored (63). Immobility was defined as floating motionless in the water except for small movements necessary to keep the head above water. Water was replaced between each trial. Two observers blind to the treatment conditions recorded the time spent immobile in the test session.

Sugar-Preference Test. Each mouse was exposed to a 1% (wt/vol) sucrose solution for 72 h followed by 12 h of water deprivation. Each mouse was then exposed to two identical bottles, one containing 1% (wt/vol) sucrose solution and the other containing water, for 1 h. Fluid intake was calculated as a preference score (percentage sucrose water preference, relative to total fluid intake).

Western Blot Assay and Coimmunoprecipitation Assay. Assays were performed as described previously (16, 20, 26, 58, 64–66). To test for proteins of similar size, we used primary antibodies raised in two different species, or the blot was stripped and reprobed. Alternatively we ran identical gels (sister gels) with the loading control for comparison.

Plasma Membrane Fractionation. The protocol for isolation of the plasma membrane fraction was based on a previous study (67), with minor modifications. Neuronal cultures were rinsed with HES buffer [20 mM Hepes (pH 7.4), 1 mM EDTA, 250 mM sucrose with protease inhibitors] and were scraped into cold HES buffer and passed through a 26-gauge needle. The nuclei were removed by centrifugation at 1,000 × g for 5 min. The supernatant was centrifuged at 100,000 × g for 60 min at 4 °C to separate the cytoplasmic fraction (supernatant) and membranous fraction (pellet). The pellet was layered onto 1.12 M sucrose in HE buffer [20 mM Hepes (pH 7.4), 1 mM EDTA, 1× Halt protease inhibitor] and centrifuged at 100,000 × g for 60 min, yielding a white fluffy band at the interface (plasma membrane). The plasma membrane fraction was resuspended in HES buffer and pelleted at 40,000 × g for 20 min. The pellets were resuspended in sample buffer, and protein concentrations were quantified.

Statistical Analysis. All experiments were repeated at least three times, and data were expressed as means ± SD. Statistical differences were analyzed by one-way ANOVA followed by multiple comparisons performed with a post hoc Bonferroni test (SPSS version 20.0; IBM). Values of *P* < 0.01 were

considered statistically significant. The significance of any differences between two groups was tested using a paired-samples *t* test when appropriate.

ACKNOWLEDGMENTS. This work was supported by National Natural Science Foundation of China Grants 81302195, 31371139, 81571282, 81771457,

81700859, 81371055, 81570859, 81502162, and 81670878, by Natural Science Foundation of Jiangsu Province Grants BK2016022104, BK20170060, and BK20172065, and in part by NIH Intramural Research Program Project Z01-ES-101643 (L.B.) and by National Institute of Neurological Disorders and Stroke Grants R01NS094440 and R21MH104252 (both to J.M.).

1. Minichiello L (2009) TrkB signalling pathways in LTP and learning. *Nat Rev Neurosci* 10:850–860.
2. Phillips C (2017) Brain-derived neurotrophic factor, depression, and physical activity: Making the neuroplastic connection. *Neural Plast* 2017:7260130.
3. Björkholm C, Monteggia LM (2016) BDNF—A key transducer of antidepressant effects. *Neuropharmacology* 102:72–79.
4. Marsden WN (2013) Synaptic plasticity in depression: Molecular, cellular and functional correlates. *Prog Neuropsychopharmacol Biol Psychiatry* 43:168–184.
5. Castrén E, Rantamäki T (2010) The role of BDNF and its receptors in depression and antidepressant drug action: Reactivation of developmental plasticity. *Dev Neurobiol* 70:289–297.
6. Watanabe Y, Gould E, McEwen BS (1992) Stress induces atrophy of apical dendrites of hippocampal CA3 pyramidal neurons. *Brain Res* 588:341–345.
7. Wohleb ES, Gerhard D, Thomas A, Duman RS (2017) Molecular and cellular mechanisms of rapid-acting antidepressants ketamine and scopolamine. *Curr Neuropharmacol* 15:11–20.
8. Arumugam V, et al. (2017) The impact of antidepressant treatment on brain-derived neurotrophic factor level: An evidence-based approach through systematic review and meta-analysis. *Indian J Pharmacol* 49:236–242.
9. Duric V, et al. (2010) A negative regulator of MAP kinase causes depressive behavior. *Nat Med* 16:1328–1332.
10. Obermeier A, et al. (1993) Identification of Trk binding sites for SHC and phosphatidylinositol 3'-kinase and formation of a multimeric signaling complex. *J Biol Chem* 268:22963–22966.
11. Yamada M, et al. (1999) Brain-derived neurotrophic factor stimulates interactions of Shp2 with phosphatidylinositol 3-kinase and Grb2 in cultured cerebral cortical neurons. *J Neurochem* 73:41–49.
12. Korhonen JM, Said FA, Wong AJ, Kaplan DR (1999) Gab1 mediates neurite outgrowth, DNA synthesis, and survival in PC12 cells. *J Biol Chem* 274:37307–37314.
13. Kaplan DR, Stephens RM (1994) Neurotrophin signal transduction by the Trk receptor. *J Neurobiol* 25:1404–1417.
14. Atwal JK, Massie B, Miller FD, Kaplan DR (2000) The TrkB-Shc site signals neuronal survival and local axon growth via MEK and P13-kinase. *Neuron* 27:265–277.
15. Patapoutian A, Reichardt LF (2001) Trk receptors: Mediators of neurotrophin action. *Curr Opin Neurobiol* 11:272–280.
16. Cao C, et al. (2009) Galpha(i1) and Galpha(i3) are required for epidermal growth factor-mediated activation of the Akt-mTORC1 pathway. *Sci Signal* 2:ra17.
17. Ghosh P, et al. (2010) A Galphai-GIV molecular complex binds epidermal growth factor receptor and determines whether cells migrate or proliferate. *Mol Biol Cell* 21:2338–2354.
18. Birnbaumer L (2007) Expansion of signal transduction by G proteins. The second 15 years or so: From 3 to 16 alpha subunits plus betagamma dimers. *Biochim Biophys Acta* 1768:772–793.
19. Suki WN, Abramowitz J, Mattera R, Codina J, Birnbaumer L (1987) The human genome encodes at least three non-allelic G proteins with alpha i-type subunits. *FEBS Lett* 220:187–192.
20. Zhang YM, et al. (2015) Requirement of Gai1/3-Gab1 signaling complex for keratinocyte growth factor-induced PI3K-AKT-mTORC1 activation. *J Invest Dermatol* 135:181–191.
21. Moscatelli I, Pierantozzi E, Camaioni A, Siracusa G, Campagnolo L (2009) p75 neurotrophin receptor is involved in proliferation of undifferentiated mouse embryonic stem cells. *Exp Cell Res* 315:3220–3232.
22. Chen J, et al. (2011) Antioxidant activity of 7,8-dihydroxyflavone provides neuroprotection against glutamate-induced toxicity. *Neurosci Lett* 499:181–185.
23. Andero R, et al. (2011) Effect of 7,8-dihydroxyflavone, a small-molecule TrkB agonist, on emotional learning. *Am J Psychiatry* 168:163–172.
24. Reichardt LF (2006) Neurotrophin-regulated signalling pathways. *Philos Trans R Soc Lond B Biol Sci* 361:1545–1564.
25. Zhou L, Talebian A, Meakin S (2015) The signaling adapter, FRS2, facilitates neuronal branching in primary cortical neurons via both Grb2- and Shp2-dependent mechanisms. *J Mol Neurosci* 55:663–677.
26. Cao C, et al. (2013) Impairment of TrkB-PSD-95 signaling in Angelman syndrome. *PLoS Biol* 11:e1001478.
27. Borghesani PR, et al. (2002) BDNF stimulates migration of cerebellar granule cells. *Development* 129:1435–1442.
28. Kokubo M, et al. (2009) BDNF-mediated cerebellar granule cell development is impaired in mice null for CaMKK2 or CaMKIV. *J Neurosci* 29:8901–8913.
29. Fu X, et al. (2011) Retrolinik cooperates with endophilin A1 to mediate BDNF-TrkB early endocytic trafficking and signaling from early endosomes. *Mol Biol Cell* 22:3684–3698.
30. Harward SC, et al. (2016) Autocrine BDNF-TrkB signalling within a single dendritic spine. *Nature* 538:99–103.
31. Park H, Poo MM (2013) Neurotrophin regulation of neural circuit development and function. *Nat Rev Neurosci* 14:7–23.
32. Yoshii A, Constantine-Paton M (2010) Postsynaptic BDNF-TrkB signaling in synapse maturation, plasticity, and disease. *Dev Neurobiol* 70:304–322.
33. Zhou QG, et al. (2011) Hippocampal neuronal nitric oxide synthase mediates the stress-related depressive behaviors of glucocorticoids by downregulating glucocorticoid receptor. *J Neurosci* 31:7579–7590.
34. Zhou QG, et al. (2011) Hippocampal telomerase is involved in the modulation of depressive behaviors. *J Neurosci* 31:12258–12269.
35. Zhou QG, et al. (2007) Neuronal nitric oxide synthase contributes to chronic stress-induced depression by suppressing hippocampal neurogenesis. *J Neurochem* 103:1843–1854.
36. Hare BD, Ghosal S, Duman RS (2017) Rapid acting antidepressants in chronic stress models: Molecular and cellular mechanisms. *Chronic Stress (Thousand Oaks)*, 1.
37. Choo M, et al. (2017) Retrograde BDNF to TrkB signaling promotes synapse elimination in the developing cerebellum. *Nat Commun* 8:195.
38. Liot G, et al. (2013) Mutant Huntingtin alters retrograde transport of TrkB receptors in striatal dendrites. *J Neurosci* 33:6298–6309.
39. Mitchell DJ, et al. (2012) Trk activation of the ERK1/2 kinase pathway stimulates intermediate chain phosphorylation and recruits cytoplasmic dynein to signaling endosomes for retrograde axonal transport. *J Neurosci* 32:15495–15510.
40. Zhou B, Cai Q, Xie Y, Sheng ZH (2012) Snapin recruits dynein to BDNF-TrkB signaling endosomes for retrograde axonal transport and is essential for dendrite growth of cortical neurons. *Cell Rep* 2:42–51.
41. Lin DC, et al. (2006) APPL1 associates with TrkA and GIPC1 and is required for nerve growth factor-mediated signal transduction. *Mol Cell Biol* 26:8928–8941.
42. Mao X, et al. (2006) APPL1 binds to adiponectin receptors and mediates adiponectin signalling and function. *Nat Cell Biol* 8:516–523.
43. McAllister AK, Katz LC, Lo DC (1996) Neurotrophin regulation of cortical dendritic growth requires activity. *Neuron* 17:1057–1064.
44. O'Neill KM, Kwon M, Donohue KE, Firestein BL (2017) Distinct effects on the dendritic arbor occur by microbead versus bath administration of brain-derived neurotrophic factor. *Cell Mol Life Sci* 74:4369–4385.
45. Dijkhuizen PA, Ghosh A (2005) BDNF regulates primary dendrite formation in cortical neurons via the PI3-kinase and MAP kinase signaling pathways. *J Neurobiol* 62:278–288.
46. Kellner Y, et al. (2014) The BDNF effects on dendritic spines of mature hippocampal neurons depend on neuronal activity. *Front Synaptic Neurosci* 6:5.
47. Gu J, Firestein BL, Zheng JQ (2008) Microtubules in dendritic spine development. *J Neurosci* 28:12120–12124.
48. Ji Y, et al. (2010) Acute and gradual increases in BDNF concentration elicit distinct signaling and functions in neurons. *Nat Neurosci* 13:302–309.
49. Tyler WJ, Pozzo-Miller LD (2001) BDNF enhances quantal neurotransmitter release and increases the number of docked vesicles at the active zones of hippocampal excitatory synapses. *J Neurosci* 21:4249–4258.
50. Hajszan T, et al. (2009) Remodeling of hippocampal spine synapses in the rat learned helplessness model of depression. *Biol Psychiatry* 65:392–400.
51. Lepack AE, Bang E, Lee B, Dwyer JM, Duman RS (2016) Fast-acting antidepressants rapidly stimulate ERK signaling and BDNF release in primary neuronal cultures. *Neuropharmacology* 111:242–252.
52. Li N, et al. (2010) mTOR-dependent synapse formation underlies the rapid antidepressant effects of NMDA antagonists. *Science* 329:959–964.
53. Nibuya M, Morinobu S, Duman RS (1995) Regulation of BDNF and trkB mRNA in rat brain by chronic electroconvulsive seizure and antidepressant drug treatments. *J Neurosci* 15:7539–7547.
54. Bessa JM, et al. (2009) The mood-improving actions of antidepressants do not depend on neurogenesis but are associated with neuronal remodeling. *Mol Psychiatry* 14:764–773, 739.
55. Chen ZY, et al. (2006) Genetic variant BDNF (Val66Met) polymorphism alters anxiety-related behavior. *Science* 314:140–143.
56. Sarkar A, et al. (2014) Hippocampal HDAC4 contributes to postnatal fluoxetine-evoked depression-like behavior. *Neuropsychopharmacology* 39:2221–2232.
57. Sharma AN, da Costa e Silva BF, Soares JC, Carvalho AF, Quevedo J (2016) Role of trophic factors GDNF, IGF-1 and VEGF in major depressive disorder: A comprehensive review of human studies. *J Affect Disord* 197:9–20.
58. Li ZW, et al. (2016) Over-expression of Galphai3 in human glioma is required for Akt-mTOR activation and cell growth. *Oncotarget*, 10.18632/oncotarget.10995.
59. Blair LA, Bence KK, Marshall J (1999) Jellyfish green fluorescent protein: A tool for studying ion channels and second-messenger signaling in neurons. *Methods Enzymol* 302:213–225.
60. Banker G, Goslin K (1988) Developments in neuronal cell culture. *Nature* 336:185–186.
61. Cao C, et al. (2006) EGFR-mediated expression of aquaporin-3 is involved in human skin fibroblast migration. *Biochem J* 400:225–234.
62. Yang H, Wang H, Jaenisch R (2014) Generating genetically modified mice using CRISPR/Cas-mediated genome engineering. *Nat Protoc* 9:1956–1968.
63. Ducottet C, Griebel G, Belzung C (2003) Effects of the selective nonpeptide corticotropin-releasing factor receptor 1 antagonist antalarmin in the chronic mild stress model of depression in mice. *Prog Neuropsychopharmacol Biol Psychiatry* 27:625–631.
64. Chen MB, et al. (2014) MicroRNA-451 regulates AMPK/mTORC1 signaling and fascin1 expression in HT-29 colorectal cancer. *Cell Signal* 26:102–109.
65. Yang L, et al. (2015) C6 ceramide dramatically enhances docetaxel-induced growth inhibition and apoptosis in cultured breast cancer cells: A mechanism study. *Exp Cell Res* 332:47–59.
66. Cai S, et al. (2017) Gai3 nuclear translocation causes irradiation resistance in human glioma cells. *Oncotarget* 8:35061–35068.
67. Defries DM, Taylor CG, Zahradka P (2016) GLUT3 is present in Clone 9 liver cells and translocates to the plasma membrane in response to insulin. *Biochem Biophys Res Commun* 477:433–439.